The Journal of Chemical Physics

Assignment of photoelectron spectra of halide–water clusters: Contrasting patterns of delocalization in Dyson orbitals

Cite as: J. Chem. Phys. **138**, 164317 (2013); https://doi.org/10.1063/1.4802251
Submitted: 26 February 2013 . Accepted: 05 April 2013 . Published Online: 25 April 2013

O. Dolgounitcheva, V. G. Zakrzewski, and J. V. Ortiz

Assignment of photoelectron spectra of halide–water clusters: Contrasting patterns of delocalization in Dyson orbitals

O. Dolgounitcheva, V. G. Zakrzewski, and J. V. Ortiz[a)]
Department of Chemistry and Biochemistry, Auburn University, Auburn, Alabama 36849-5312, USA

(Received 26 February 2013; accepted 5 April 2013; published online 25 April 2013)

Ab initio electron propagator calculations in various self-energy approximations provide accurate assignments of peaks observed in the photoelectron spectra of complexes that comprise a fluoride or chloride anion and two or three water molecules. More than one minimum structure is found in all four cases. When the halide anion is Cl^-, the first three final states may be described as quasi-degenerate ^{2}P chlorine atoms coordinated to water molecules. Higher final states consist of a chloride anion juxtaposed to a positive charge that is delocalized over the water molecules. For the clusters with fluoride anions, most of the final states correspond to Dyson orbitals that are delocalized over the F and O nuclei. A variety of F–O σ and π bonding and antibonding patterns are evident in the Dyson orbitals. The assignment of low-lying spectral peaks to halide p orbital vacancies or to delocalized solvent orbitals is more valid for the chloride clusters than for the fluoride clusters, where a delocalized picture arises from strong bonding interactions between F $2p$ and H_2O $1b_1$ orbitals. [http://dx.doi.org/10.1063/1.4802251]

INTRODUCTION

Electron photodetachment from anions embedded in solvent molecules,[1–5] whether in gas-phase clusters or near the surface of a liquid droplet, is capable of producing final states with vacancies in localized or delocalized orbitals that are occupied in the initial state. For gas-phase halide complexes with water molecules, localized final states may be described as solvated ^{2}P halogen atoms or as ^{1}S halide anions that are juxtaposed to a positive charge that may be spread over many water molecules. Delocalized vacancies that correspond to the latter case contrast with the localized holes of the former case. If the lowest electron detachment energies are ascribed to final states with an uncharged halide radical, higher transition energies must be assigned to states that exhibit an electron transfer to the halogen atom from the solvent molecules. Such states may be regarded as molecular precursors of condensed-phase systems in which (positive) charge transfer (from solute) to solvent (CTTS) has occurred.

Halide–water clusters have been amply examined with the tools of *ab initio* molecular electronic structure theory.[6–13] These studies have identified alternative structures and corresponding binding energies of water molecules. Relative energies of minima in which halide anions occupy interior or exterior positions have been scrutinized.

Complexes of the chloride anion with ammonia or water molecules have been studied experimentally and computationally.[14] To interpret the photoelectron spectrum of $[Cl^-(NH_3)]$, coupled-cluster calculations were performed. A sharp, intense feature with a photodetachment energy of approximately 4 eV was followed by a broader, less intense peak from 6.0 to 6.8 eV. The former peak was assigned to final states with a vacancy in one of three Cl $3p$ orbitals split by the presence of the ammonia molecule. To the band centered around 6.4 eV, a state with a vacancy in the highest occupied molecular orbital of NH_3 was assigned. A qualitative description of this state, $[Cl^-(NH_3^+)]$, suggests that it is a precursor to a CTTS final state. Subsequent photoelectron studies of $[Cl^-(H_2O)_n]$ clusters with $n = 0$–7[15] presented spectra in which the lowest transition energies increased with n and were assigned to electron detachment from a chloride anion.

Another set of coupled-cluster calculations was performed on complexes that comprise a single halide (F^- or Cl^-) and a single solvent molecule (H_2O or NH_3).[16] In all four complexes, the first three electron detachment energies were assigned to three, closely spaced states with vacancies in one of three halide p orbitals and the fourth transition energy was assigned to a charge-transfer state with a positive charge localized on the solvent molecule.

Electrospray anion photoelectron experiments on $[F^-(H_2O)_n]$ complexes with $n = 1$–4[17] displayed threshold detachment energies that increased with the number of water molecules. For the three smallest clusters, two separated band maxima appeared. For $n = 1$, a broad band with a peak near 4.8 eV was assigned to detachment from a fluoride anion and the next peak, near 6.1 eV, was attributed to a charge-transfer final state. Similar patterns were observed for $n = 2$, 3, but with both peaks shifted to higher transition energies. In addition, the relative intensities of the second peaks were greater with higher n. For the $n = 4$ cluster, only a single, broad feature that extended beyond the photon energy was observed.

Electron propagator calculations in the third-order algebraic diagrammatic construction, or ADC(3), approximation[18] were performed for the same fluoride–water clusters through $n = 3$.[19] With an augmented, double-ζ plus polarization basis set, this procedure overestimated the electron affinity of F by about 0.6 eV and led to similar

a)ortiz@auburn.edu.

overestimates for the lowest electron detachment energies of the cluster with $n = 1$. ADC methods that are consistent through fourth order may be needed to achieve better results for the electron affinity of F. Final states were characterized qualitatively as having orbital vacancies in F $2p$ orbitals or water molecular orbitals. Similar results were obtained for clusters with $n = 2, 3$.

A recent study of basis set and correlation effects in electron propagator calculations on the $[F^-(H_2O)]$ and $[Cl^-(H_2O)]$ complexes concluded that certain diagonal self-energy approximations in combination with basis sets of triple-ζ quality with polarization and diffuse functions are capable of producing accurate electron binding energies of free and coordinated halide anions and of water molecules that are coordinated to an anion.[20] This work also produced a delocalized picture of the orbital vacancies created by photodetachment for most of the final states in the fluoride complex. However, a localized picture for the lowest final states emerged from calculations on $[Cl^-(H_2O)]$.

The most efficient of the electron propagator methods found to have predictive quality in the previous work[20] were employed in calculations on a $[F^-(H_2O)_6]$ cluster embedded in solvent configurations generated by a Monte-Carlo simulation with classical potentials.[21] This quantum-classical model of the aqueous fluoride anion obtained good agreement with photoelectron spectra on droplets of aqueous alkali–fluoride solutions. It also indicated that extensive delocalization between fluoride and water basis functions is typical of most of the orbitals that pertain to electron detachment in the valence region.

Another approach to the electronic structure of aqueous fluoride and chloride anions employed continuum solvation models in which the solute is a hexacoordinate halide anion.[22] Solvation models may cause large shifts in predicted electron binding energies. However, they also confirm the qualitative conclusions on the degree of delocalization of orbital vacancies that were reached in the two previous studies.[20,21]

On the basis of these successful methodological tests,[20–22] electron binding energies of the $[F^-(H_2O)_2]$, $[F^-(H_2O)_3]$, $[Cl^-(H_2O)_2]$, and $[Cl^-(H_2O)_3]$ complexes are determined with electron propagator methods and assigned to features observed in anion photoelectron spectra.[17] Changes in electronic structure corresponding to various final states are interpreted in terms of orbital concepts.

METHODS

Theory

For every electron binding energy (e.g., ionization energy of a molecule, electron affinity of a molecule, electron detachment energy of an anion), there is a corresponding Dyson orbital (DO), which may be regarded as an overlap function that involves the many-electron wavefunctions of the initial and final states. (Electron propagator theory describes relationships between electron binding energies and Dyson orbitals.[23–26]) For the case of the vertical electron detachment energy (VEDE) of a ground-state anion with N electrons, the xth Dyson orbital reads

$$\Phi_x^{Dyson}(z_1) = \sqrt{N} \int \Psi_{anion}(z_1, z_2, z_3, ..., z_N) \Psi^*_{neutral,x}(z_2, z_3, z_4, ..., z_N) dz_2 dz_3 dz_4 ... dz_N, \quad (1)$$

where z_t is the space-spin coordinate of the tth electron. Phase information is present in the DO, which is capable of displaying bonding, antibonding, and nonbonding relationships between constituent atomic basis functions. DOs are not generally normalized to unity. In fact, their norms, known as pole strengths, read

$$P_x = \int \left|\Phi_x^{Dyson}(z_t)\right|^2 dz_t \quad (2)$$

and may have values between zero and unity. Pole strengths are qualitative indices of the importance of correlation effects in describing an electron attachment or detachment. In the Hartree–Fock (HF) or Koopmans's theorem (KT) description of transitions between an initial state, described by a variationally optimized Slater determinantal wavefunction, and a final state whose Slater-determinantal wavefunction is constructed from frozen orbitals, DOs are equivalent to canonical, HF orbitals and their pole strengths equal unity. However, for transitions from the same HF initial state to a so-called shakeup state in which two vacancies in initially occupied, frozen orbitals and an electron in a corresponding unoccupied orbital are present, the pole strength vanishes. In calculations that consider orbital relaxation in final states and the effects of electron correlation, pole strengths generally lie between these two extremes.

Electron propagator methods employed in the present work are based on the Dyson equation. The quasiparticle form of this equation:

$$[F + \Sigma(\epsilon_x)]\Phi_x^{Dyson} = \epsilon_x \Phi_x^{Dyson}, \quad (3)$$

where F is a generalized Fock operator that depends on a reference one-electron density matrix, $\Sigma(E)$ is the self-energy operator that describes relaxation and correlation effects, and ϵ_x is the xth electron binding energy, is a generalization of the canonical form of the HF equations, in which the xth orbital energy is associated with the xth canonical orbital. In the generalization provided by the Dyson equation, correlated electron binding energies are mapped to correlated DOs. The self-energy operator may be systematically improved up to the exact limit, which produces exact electron binding energies and DOs as solutions of the corresponding Dyson equation.

Several approximations used in this work employ perturbative expressions for the self-energy matrix elements that are based on canonical HF orbitals and energies. In addition, these approximations neglect off-diagonal matrix elements of $\Sigma(E)$ in the canonical, HF basis. Therefore, the DOs in these diagonal self-energy approximations have a simple form in which

$$\Phi_x^{Dyson} = \sqrt{P_x}\Phi_x^{CHF}, \quad (4)$$

where Φ_x^{CHF} is the xth, canonical, HF orbital. Contour plots of DOs in these approximations differ from those of canonical, HF orbitals only by a factor of $\sqrt{P_x}$.

TABLE I. $[F^-(H_2O)_2]$ total (a.u.) and relative (kcal/mol) energies.

	MP2					
	6-311++G**			6-311++G(2*df*,2*p*)		
Structure	E_{MP2}	ΔE_{MP2}	N_i	E_{MP2}	ΔE_{MP2}	N_i
C_2	− 252.30703	0	0	− 252.43539	0	0
C_{2v}	− 252.30629	0.46	2	− 252.43431	0.68	2
C'_{2v}	− 252.30650	0.33	1	− 252.43410	0.81	2
C_{2h}	− 252.30625	0.49	2	− 252.43452	0.54	1

	BD(full)							
	6-311++G**				6-311++G(2*df*,2*p*)			
Structure	E_{BD}	ΔE_{BD}	N_i	ΔE_{BD+ZPE}	E_{BD}	ΔE_{BD}	N_i	ΔE_{BD+ZPE}
C_2	− 252.36989	0	0	0	− 252.50371	0	0	0
C_{2v}	− 252.36921	0.43	0	0.53	− 252.50274	0.61	0	0.13
C'_{2v}	− 252.36943	0.29	0	0.48	− 252.50266	0.66	0	0.23
C_{2h}	− 252.36928	0.38	2		− 252.50314	0.36	0	− 0.04

A more powerful and flexible approach (the BD-T1 self-energy approximation[23,24,26]) produces DOs as a linear combination of semicanonical Brueckner (SB) orbitals that result from Brueckner doubles (BD) coupled-cluster calculations,[27] where

$$\Phi_x^{Dyson} = \sum_q \Phi_q^{SB} C_{qx}^{SB}, \tag{5}$$

and where q is a general orbital index. (SB orbitals diagonalize the occupied–occupied and virtual–virtual blocks of the Fock matrix, but produce nonzero elements in the occupied–virtual and virtual–occupied blocks.) The resulting Dyson orbitals may be compared with their counterparts from diagonal self-energy calculations based on HF orbitals and energies.

Computational details

The developers' version of the Gaussian suite of codes[28] was employed in the present calculations. Equilibrium geometries of anionic complexes were optimized with second-order (MP2) and BD total energies obtained with the 6-311++G** or 6-311++G(2*df*,2*p*) basis sets.[29] VEDEs were calculated with the following electron propagator methods: Outer-Valence Green's Function (OVGF),[18,30] partial third order (P3),[31,32] renormalized partial third order (P3+),[33] and Brueckner-doubles, triple field-operator approximation (BD-T1).[23] (The first three methods employ the diagonal self-energy approximation in the canonical, HF orbital basis.) The 6-311++G(2*df*,*p*) basis was used in the electron propagator calculations. All pole strengths exceeded 0.90. Structures of the clusters and molecular contour plots were generated with the MOLDEN graphing package.[34] The values of the contours are ±0.03.

RESULTS AND DISCUSSION

$F^-(H_2O)_2$

Total and relative energies of four isomers of $F^-(H_2O)_2$ obtained with the MP2 and BD methods are compiled in Table I. (For each optimized structure, the number of imaginary frequencies is listed in the column labeled N_i.) The corresponding structures are presented in Fig. 1. Four initial configurations were taken from a recent computational study.[6] A C_1 initial geometry with hydrogen bonds between the two water molecules as well as between the fluoride and the water molecules converged to the C_2 structure. Whereas MP2 optimizations produce only one, C_2 minimum, BD/6–311++G(2*df*,2*p*) predicts four minima. For both methods, the potential energy surface is very flat, for the largest energy difference between minima does not exceed 0.7 kcal/mol. When corrections for zero-point energy (ZPE) are taken into account, the largest difference is less than 0.3 kcal/mol. At the BD/6-311++G(2*df*,2*p*) level, the C_{2h} structure is the lowest and the C_2 isomer is second lowest when ZPE corrections are included.

VEDEs and coefficients of semicanonical Brueckner (SB) orbitals in the Dyson orbitals, C_q^{SB}, are compiled in Table II. OVGF, P3, and P3+ data are presented in Table III.

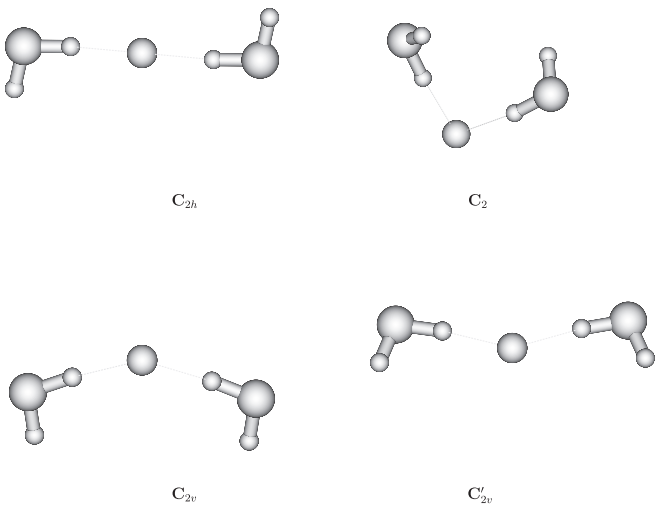

FIG. 1. Isomers of $[F^-(H_2O)_2]$.

TABLE II. $[F^-(H_2O)_2]$ BD-T1 VEDEs (eV).

C_{2h} structure				C_2 structure				Expt.
State	VEDE	C_q^{SB}	q	State	VEDE	C_q^{SB}	q	Ref. 17
X^2B_u	5.97	0.99	12	X^2B	6.09	0.85	12	5.79 ± 10
						0.42	10	
						0.30	8	
A^2A_u	6.10	0.88	11	A^2A	6.08	0.92	11	
		−0.48	8			0.37	9	
B^2B_u	6.36	1.00	9	B^2B	6.09	0.85	12	
						0.42	10	
						0.30	8	
C^2B_g	6.69	1.00	10	C^2A	6.80	0.92	9	6.80 ± 10
						−0.38	11	
D^2A_u	6.92	0.87	8	D^2B	6.81	0.80	8	6.80 ± 10
		0.48	11			0.37	10	
						−0.47	12	
E^2A_g	8.97	1.00	7	E^2B	9.24	0.99	7	
C_{2v} structure				C'_{2v} structure				Expt.
State	VEDE	C_q^{SB}	q	State	VEDE	C_q^{SB}	q	Ref. 17
X^2B_2	6.05	0.99	12	X^2B_2	5.96	1.00	12	5.79 ± 10
A^2B_1	6.12	0.87	11	A^2B_1	6.10	0.88	11	
		−0.48	8			−0.48	8	
B^2A_1	6.27	1.00	9	B^2A_1	6.37	1.00	9	
C^2A_2	6.74	1.00	10	C^2A_2	6.67	1.00	10	6.80 ± 10
D^2B_1	6.94	0.87	8	D^2B_1	6.94	0.87	8	6.80 ± 10
		0.48	11			0.48	11	
E^2A_1	9.12	0.99	7	E^2A_1	9.12	0.99	7	

TABLE III. $[F^-(H_2O)_2]$ VEDEs (eV).

		OVGF					Expt.
State	KT	A	B	C	P3	P3+	Ref. 17
			C_{2h} structure				
X^2B_u	7.55	6.24	6.64	6.51	6.12	5.82	5.79 ± 10
A^2A_u	7.79	6.40	6.76	6.66	6.30	6.01	
B^2B_u	8.13	6.76	7.23	7.01	6.51	6.13	
C^2B_g	8.16	6.79	7.02	7.03	6.85	6.64	6.80 ± 10
D^2A_u	8.51	7.13	7.49	7.39	7.04	6.74	6.80 ± 10
E^2A_g	10.31	9.07	9.33	9.33	9.11	8.90	
			C_2 structure				
X^2A	7.74	6.39	6.81	6.66	6.22	5.90	5.79 ± 10
A^2B	7.74	6.39	6.79	6.66	6.25	5.94	
B^2B	7.94	6.57	6.95	6.83	6.44	6.14	
C^2A	8.29	6.91	7.15	7.15	6.96	6.74	6.80 ± 10
D^2B	8.40	7.02	7.38	7.28	6.93	6.63	
E^2B	10.65	9.39	9.68	9.65	9.40	9.17	
			C_{2v} structure				
X^2B_2	7.63	6.32	6.73	6.60	6.19	5.89	5.79 ± 10
A^2B_1	7.81	6.42	6.78	6.68	6.32	6.02	
B^2A_1	8.02	6.65	7.12	6.91	6.42	6.06	
C^2A_2	8.19	6.82	7.05	7.06	6.88	6.67	6.80 ± 10
D^2B_1	8.53	7.16	7.51	7.41	7.06	6.77	6.80 ± 10
E^2A_1	10.50	9.25	9.53	9.51	9.27	9.04	
			C'_{2v} structure				
X^2B_2	7.55	6.23	6.63	6.50	6.10	5.81	5.79 ± 10
A^2B_1	7.78	6.38	6.74	6.65	6.30	6.01	
B^2A_1	8.12	6.75	7.22	7.01	6.50	6.14	
C^2A_2	8.14	6.77	6.99	7.00	6.82	6.61	6.80 ± 10
D^2B_1	8.50	7.12	7.49	7.38	7.01	6.71	6.80 ± 10
E^2A_1	10.30	9.05	9.32	9.32	9.09	8.88	

In all cases, the pole strengths exceed 0.90 and therefore validate the diagonal self-energy approximation used in the three latter methods.

C_{2h} structure

The VEDE for the first final state, X^2B_u, is predicted by BD-T1 to be 5.97 eV and is in a good agreement with the centroid of the first band in the spectrum.[17] This transition is followed by VEDEs for the A^2A_u state at 6.10 eV and for the B^2B_u state at 6.36 eV. Both energies fit well into the first band of the experimental spectrum and are close to a peak that occurs near 6.2 eV. The C^2B_g state and the D^2A_u state are predicted at VEDEs of 6.69 eV and 6.92 eV, respectively. Both values are in very good agreement with the centroid of the second band in the experimental spectrum at 6.80 ± 0.10 eV. The last BD-T1 VEDE, 8.97 eV, is beyond the range of the light source.

Dyson orbitals corresponding to ^2B_u, ^2B_g, and ^2A_g final states have only one important component in the basis of SB orbitals. For the A and D final states of ^2A_u symmetry, two SB orbitals contribute significantly to the DOs. This interference of SB orbitals produces DOs that closely resemble canonical, HF orbitals.

Among the electron propagator approximations of Table III, the P3+ energies are in the best agreement with experimental data for the X, C, and D states and practically coincide with the reported centroids of two bands. Results for the A and B states also are in close agreement with the local maximum near 6.2 eV that is seen in the spectrum. For the A and B states, P3+ predictions are lower than corresponding BD-T1 results. All three OVGF approximations and the P3 method produce higher VEDE values.

Canonical, HF orbitals are depicted in Fig. 2. (The highest occupied SB orbitals are very similar for the $6b_u$, $5b_u$, $1b_g$, and $6a_g$ cases.) Anti-bonding patterns between F and O $2p$ orbitals aligned with hydrogen bonds occur for $6b_u$. The next, $2a_u$ orbital, has π character and involves $1b_1$ (highest occupied) orbitals of both H_2O molecules. In the canonical, HF orbital, contributions from each nonhydrogen atom become comparable. (The $2a_u$ SB orbital has noticeably larger oxygen than fluorine contributions.) The third, $5b_u$ orbital, is localized on the fluorine atom. Only $2p$ functions on the oxygen atoms (i.e., H_2O $1b_1$ orbitals) contribute to the $1b_g$ orbital in an anti-bonding pattern. The lower-lying, $1a_u$ orbital, has π character and is a bonding counterpart to the upper orbital of the same symmetry. (The F $2p$ contribution is larger but not dominant in the $1a_u$ SB orbital.) For the a_u cases, interference of SB orbitals yields DOs that closely resemble canonical HF orbitals. The $6a_g$ orbital is an out-of-phase combination of lone-pairs lobes (i.e., $3a_1$ H_2O orbitals) of two, separate water molecules.

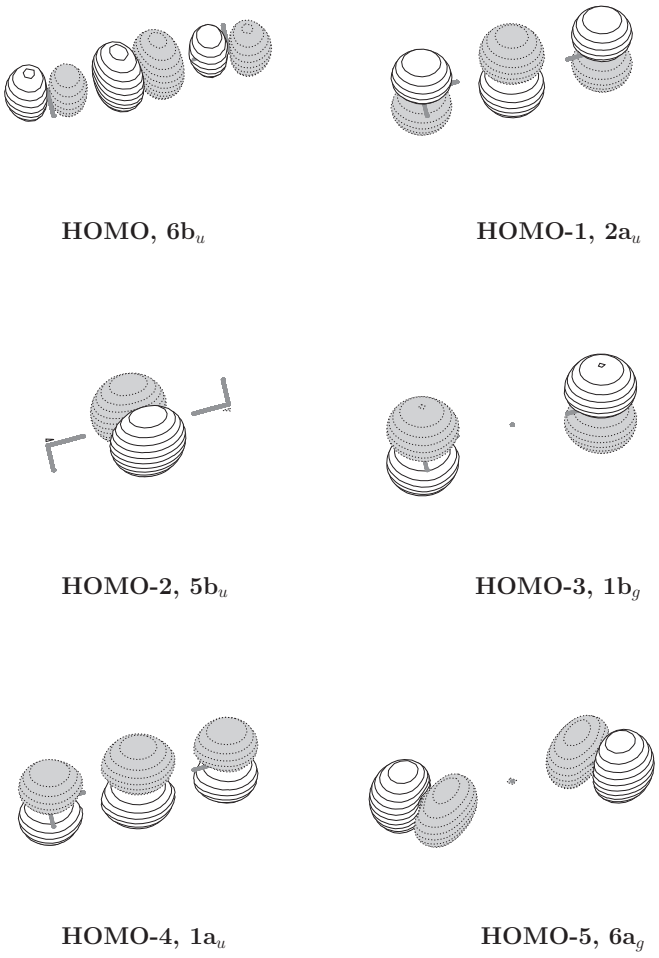

FIG. 2. Canonical Hartree–Fock orbitals of $[F^-(H_2O)_2]$ C_{2h} isomer.

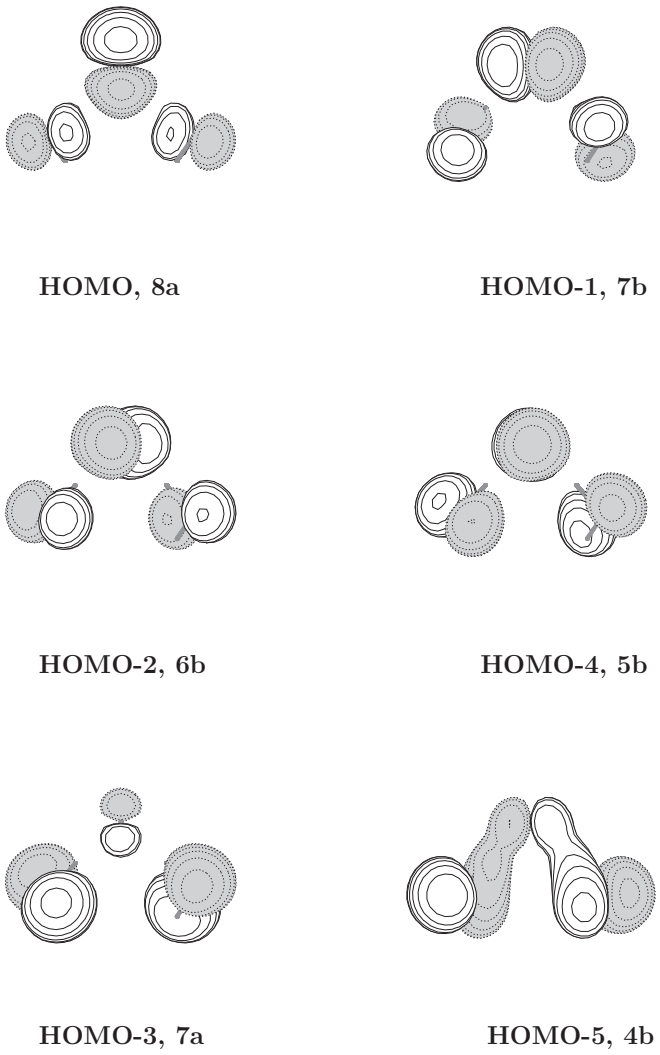

FIG. 3. Canonical Hartree–Fock orbitals of $[F^-(H_2O)_2]$ C_2 isomer.

C_2 structure

Closely spaced VEDEs are obtained for the first three final states of the C_2 isomer. In Table II, VEDEs of 6.08–6.09 eV fit well into the first band of the experimental spectrum.[17] The next two final states of A and B symmetry are predicted at 6.80 eV and 6.81 eV and correspond to the centroid of the second band of the spectrum. The E^2B state is predicted to lie beyond the range of the spectrum at 9.24 eV. For all DOs, except for the case of the largest VEDE, more than one SB orbital has a large coefficient.

Electron propagator results with diagonal self-energies in the HF basis are compiled in the second block of Table III. Once again, the OVGF energies are much larger than either BD-T1 data or experimental peak positions. Much better results are obtained with the P3 and, especially, the P3+ methods. Quasi-degeneracy of the first three final states, obtained with BD-T1, is no longer observed in the P3 or P3+ results. The first two P3+ energies are almost within experimental error. The two lower lying states at 6.63 eV and 6.74 eV (note the altered order of states in the P3 and P3+ columns) are also very close to the second band peak observed at 6.80 $\pm$ 0.10 eV.

Graphical representations of canonical, HF orbitals are given in Fig. 3. DOs constructed as linear combinations of SB orbitals (see Table II) bear a strong resemblance to canonical HF orbitals. Unlike the case of the C_{2h} structure, there are no orbitals that are exclusively localized on the fluorine or oxygen atoms.

For a similar structure, electron propagator calculations with a smaller basis were carried out in the ADC(3) approximation with a reduced operator manifold.[19] The three lowest VEDEs were ascribed to functions on the fluoride anion and six higher VEDEs were assigned to oxygen functions. In general, the results were higher than those obtained with the BD-T1 and P3+ methods.

C_{2v} structures

VEDE values obtained for both C_{2v} structures are slightly shifted with respect to those discussed above and may contribute to the observed spectral peaks. SB orbitals strongly resemble their canonical, HF counterparts except in the b_1 cases. Interference between SB orbitals produces DOs for the $^2B_1$ final states that also resemble canonical, HF orbitals (see Figs. 4 and 5). Antibonding σ relationships between O and F atoms are seen again in the DO for the lowest VEDE in both structures. For the first two VEDEs, the DOs have larger F

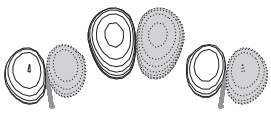

HOMO, $5b_2$

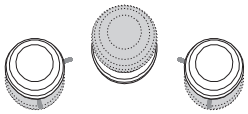

HOMO-1, $2b_1$

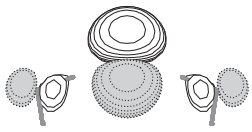

HOMO-2, $6a_1$

HOMO-3, $1a_2$

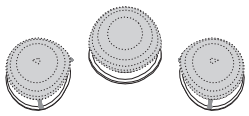

HOMO-4, $1b_1$

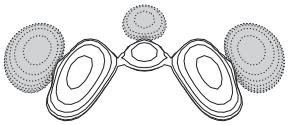

HOMO-5, $5a_1$

FIG. 4. Canonical Hartree–Fock orbitals of $[F^-(H_2O)_2]$ C_{2v} isomer.

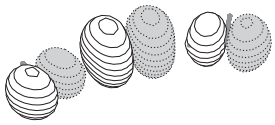

HOMO, $5b_2$

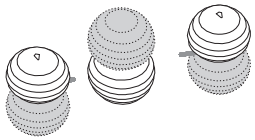

HOMO-1, $2b_1$

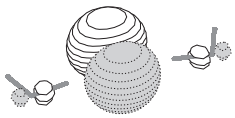

HOMO-2, $6a_1$

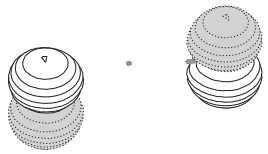

HOMO-3, $1a_2$

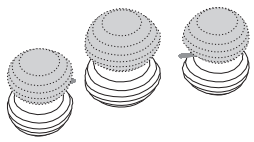

HOMO-4, $1b_1$

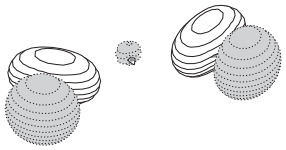

HOMO-5, $5a_1$

FIG. 5. Canonical Hartree–Fock orbitals of $[F^-(H_2O)_2]$ C'_{2v} isomer.

than O contributions, but delocalization onto O remains significant. The lower lying, $6a_1$ orbital is localized chiefly on the F atom. The $1a_2$ orbital is delocalized over two oxygen atoms and therefore is related to a charge-transfer final state. In both C_{2v} structures, three DOs are formed from a F $2p$ orbital and two H_2O $1b_1$ molecular orbitals.

$[Cl^-(H_2O)_2]$

Five close-lying structures were found for $[Cl^-(H_2O)_2]$. Table IV presents results of optimizations performed with MP2 and BD. Molecular structures of C_1, C_2, C_{2v}, and C_{2h} symmetries are displayed in Fig. 6. MP2 finds only one minimum, the C_1 structure. BD calculations predict all five structures to be minima on a relatively flat potential energy surface. The C_1 structure is the global minimum although the C_2 structure is only 0.22 kcal/mol higher. The C_{2h} structure is predicted as the third lowest when ZPE corrections are included.

BD-T1 VEDEs of all five isomers of $[Cl^-(H_2O)_2]$ are compiled in Table V. These results are in excellent agreement with the experimental band centroid of 4.97 eV.[15] For all structures, the first three VEDEs are slightly split and pertain to electron detachment from the chloride anion. The last two states (C and D) are well separated from the first band and correspond to DOs formed by H_2O $1b_1$ molecular orbitals. No experimental data are available for these two VEDEs.

OVGF, P3, and P3+ VEDEs are given in Table VI. The trends observed in these data are similar to those in

TABLE IV. $[Cl^-(H_2O)_2]$ total (a.u.) and relative (kcal/mol) energies.

	MP2					
	6-311++G**			6-311++G(2*df*,2*p*)		
Structure	E_{MP2}	ΔE_{MP2}	N_i	E_{MP2}	ΔE_{MP2}	N_i
C_1	−612.30316	0	0	−612.43918	0	0
C_2	−612.30206	0.69	1	−612.43857	0.38	1
C_{2v}	–612.30019	1.86	2	−612.43601	1.99	2
C'_{2v}	−612.30034	1.77	2	−612.43591	2.05	2
C_{2h}	−612.29905	2.58	3	−612.43573	2.16	3

	BD(full)			
	6-311++G(2*df*,2*p*)			
Structure	E_{BD}	ΔE_{BD}	i	ΔE_{BD+ZPE}
C_1	−612.56667	0	0	0
C_2	−612.56617	0.31	0	0.22
C_{2v}	−612.56388	1.75	0	0.97
C'_{2v}	−612.56380	1.80	0	1.04
C_{2h}	−612.56373	1.84	0	0.65

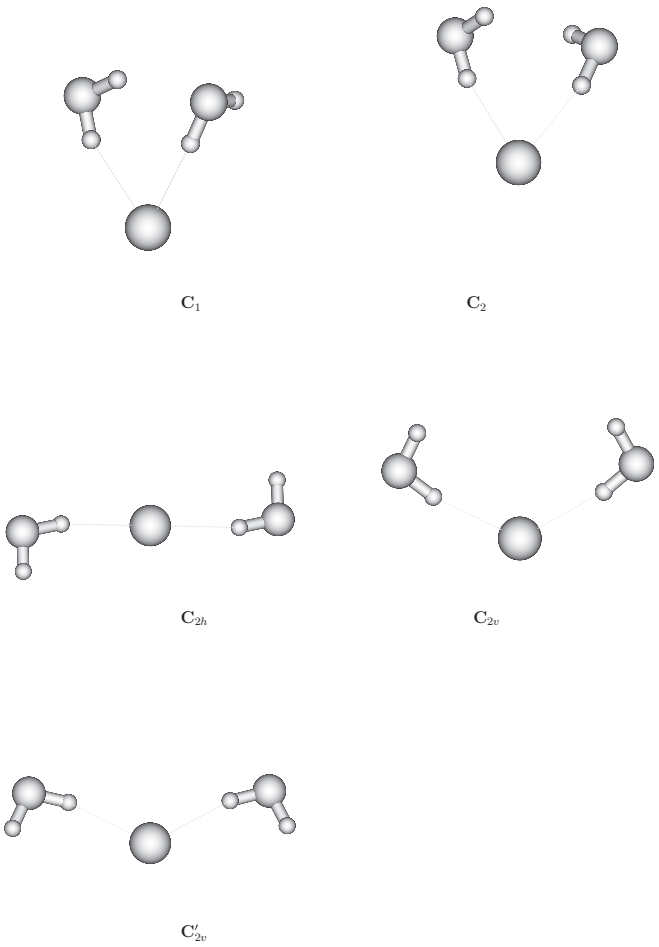

FIG. 6. Isomers of $[Cl^-(H_2O)_2]$.

Table V. All three methods predict slight splitting in the first three states of all isomers of $[Cl^-(H_2O)_2]$. OVGF results are closer to those of BD-T1 and to the experimental peak position. The P3 and the P3+ energies are somewhat lower but still within the range of the experimental band.[15]

$[F^-(H_2O)_3]$

Three minima were found in optimizations (see Fig. 7). Their total and relative energies obtained with the MP2 and BD methods are presented in Table VII. MP2 predicts two minima, the C_3 and C_s structures, while all three structures are minima at the BD level. At this level, when zero-point corrections are accounted for, the C_{3h} structure becomes the global minimum. In the two lowest structures, all three molecules of water are coordinated by the fluoride anion. The C_s isomer differs in the coordination pattern: fluoride is linked to only two water molecules while the third water molecule forms two H-bonds with the other two. Electron propagator results for $[F^-(H_2O)_3]$ C_{3h} and C_3 structures are compiled in Table VIII together with experimental data.[17]

C_3 structure

P3+ results are in best agreement with the band centroids of the experimental spectrum.[17] (P3 and OVGF VEDEs

TABLE V. $[Cl^-(H_2O)_2]$ BD-T1 VEDEs (eV).

C_1 structure				C_2 structure				
State	VEDE	C_q^{SB}	q	State	VEDE	C_q^{SB}	q	Expt. (Ref. 15)
X^2A	4.85	1.00	12	X^2B	4.86	1.00	12	4.97
A^2A	4.89	1.00	11	A^2B	4.94	1.00	11	
B^2A	4.95	0.98	10	B^2A	4.95	1.00	10	
		0.14	11					
C^2A	7.36	1.00	9	C^2B	7.53	1.00	9	
D^2A	7.83	1.00	8	D^2A	7.85	1.00	8	
C_{2h} structure				C_{2v} structure				
State	VEDE	C_q^{SB}	q	State	VEDE	C_q^{SB}	q	
X^2A_u	4.84	1.00	12	X^2B_1	4.85	1.00	12	
A^2B_u	4.88	1.00	11	A^2A_1	4.92	1.00	11	
B^2B_u	5.02	1.00	10	B^2B_2	5.02	1.00	10	
C^2B_g	7.70	1.00	9	C^2A_2	7.71	1.00	9	
D^2A_u	7.71	1.00	8	D^2B_1	7.72	1.00	8	
C'_{2v} structure								
State	VEDE	C_q^{SB}	q					
X^2A_u	4.85	1.00	12					
A^2B_u	4.94	1.00	11					
B^2B_u	4.99	1.00	10					
C^2B_g	7.65	1.00	9					
D^2A_u	7.67	1.00	8					

TABLE VI. $[Cl^-(H_2O)_2]$ VEDEs (eV).

			OVGF					Expt.
Structure	State	KT	A	B	C	P3	P3+	Ref. 15
C_1	X^2A	5.46	4.74	4.90	4.92	4.71	4.67	4.97
	A^2A	5.53	4.80	4.95	4.96	4.77	4.73	
	B^2A	5.61	4.85	5.00	5.02	4.83	4.79	
	C^2A	8.97	7.48	7.69	7.71	7.50	7.31	
	D^2A	9.51	7.97	8.17	8.19	7.99	7.79	
C_2	X^2B	5.48	4.77	4.92	4.93	4.72	4.69	
	A^2B	5.57	4.84	4.99	5.01	4.82	4.78	
	B^2A	5.62	4.86	5.00	5.02	5.12	5.00	
	C^2B	9.18	7.67	7.87	7.89	7.69	7.50	
	D^2A	9.48	7.99	8.19	8.21	8.01	7.81	
C_{2h}	X^2A_u	5.48	4.74	4.90	4.91	4.72	4.68	
	A^2B_u	5.51	4.79	4.94	4.95	4.76	4.72	
	B^2B_u	5.73	4.94	5.08	5.10	4.93	4.89	
	C^2B_g	9.29	7.82	8.04	8.05	7.85	7.65	
	D^2A_u	9.30	7.83	8.05	8.06	7.86	7.66	
C_{2v}	X^2B_1	5.48	4.76	4.91	4.93	4.72	4.68	
	A^2A_1	5.56	4.82	4.97	4.99	4.79	4.75	
	B^2B_2	5.69	4.93	5.07	5.09	4.91	4.87	
	C^2A_2	9.31	7.84	8.05	8.06	7.86	7.66	
	D^2B_1	9.32	7.85	8.06	8.08	7.88	7.68	
C'_{2v}	X^2B_1	5.48	4.76	4.91	4.92	4.72	4.68	
	A^2A_1	5.57	4.84	4.99	5.01	4.81	4.77	
	B^2B_2	5.68	4.90	5.04	5.07	4.88	4.84	
	C^2A_2	9.25	7.78	7.99	8.01	7.80	7.60	
	D^2B_1	9.26	7.79	8.00	8.02	7.81	7.62	

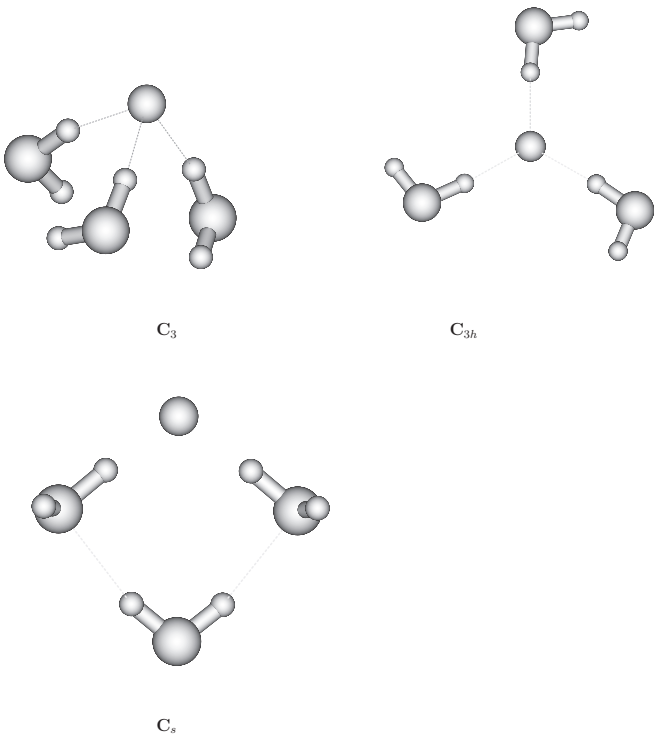

FIG. 7. Isomers of $[F^-(H_2O)_3]$.

TABLE VII. $[F^-(H_2O)_3]$ total (a.u.) and relative (kcal/mol) energies.

	MP2/6-311++G(2*df*,2*p*)			
Structure	E_{MP2}	ΔE_{MP2}	N_i	ΔE_{ZPE}
C_3	− 328.78069	0	0	0
C_{3h}	− 328.77845	1.40	1	
C_s	− 328.77851	1.36	0	1.06
	BD/6-311++G(2*df*,2*p*)			
Structure	E_{BD}	ΔE_{BD}	N_i	ΔE_{ZPE}
C_3	− 328.87567	0	0	0
C_{3h}	− 328.87381	1.17	0	− 0.24
C_s	− 328.87282	1.79	0	1.45

TABLE VIII. $[F^-(H_2O)_3]$ VEDEs (eV).

		OVGF					Expt.
State	KT	A	B	C	P3	P3+	Ref. 17
			C_3 structure				
X^2A	8.60	7.15	7.55	7.41	6.98	6.67	6.59 ± 10
A^2E	8.66	7.22	7.53	7.47	7.14	6.88	
B^2E	8.86	7.42	7.75	7.68	7.34	7.07	
C^2A	8.97	7.55	7.80	7.79	7.56	7.35	7.32 ± 10
D^2E	11.32	9.99	10.27	10.25	9.98	9.77	
			C_{3h} structure				
X^2A''	8.53	7.11	7.39	7.36	7.08	6.84	6.59 ± 10
B^2E''	8.74	7.36	7.58	7.59	7.40	7.20	7.32 ± 10
A^2E'	8.74	7.32	7.72	7.58	7.13	6.84	6.59 ± 10
C^2A''	9.44	7.96	8.38	8.21	7.73	7.40	7.32 ± 10
D^2A'	10.88	9.63	9.90	9.89	9.66	9.47	

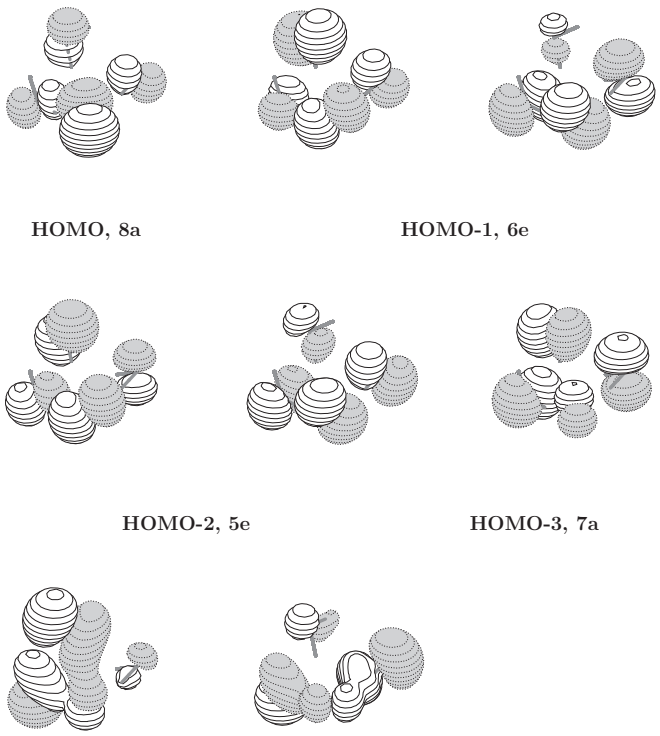

FIG. 8. Canonical Hartree–Fock orbitals of $[F^-(H_2O)_3]$ C_3 isomer.

are larger.) The VEDE for the X^2A final state is predicted at 6.67 eV by P3+. This result is very close to the experimental value of 6.59 ± 0.10 eV. The next two final states (A and B) have E symmetry and are predicted to lie well within the boundaries of the first experimental band, which has several features up to 7.0 eV.[17] Excellent agreement is achieved between the P3 energy value of 7.35 eV and the centroid of the second band in the spectrum of $[F^-(H_2O)_3]$. DOs of the C_3 isomer of $[F^-(H_2O)_3]$ are depicted in Fig. 8. The canonical, HF orbital for the lowest VEDE, Fig. 8(a), is delocalized over all four nonhydrogen nuclei and displays antibonding F–O relationships. A F 2*p* function is the most important contribution to this orbital. The rest of the DOs under consideration also are delocalized over all four constituents of the complex.

A similar structure was considered in electron propagator calculations performed with the ADC(3) approximation.[19] Three VEDEs above 7 eV were assigned to fluoride orbitals and three higher VEDEs at 7.5–7.6 eV were assigned to oxygen orbitals.

C_{3h} structure

The best correspondence with experiment[17] is achieved again by the P3+ method (see Table VIII). Here, the two first states, $^2A''$ and $^2E'$, are nearly degenerate, especially in P3+ calculations. The P3+ energy of 6.84 eV fits well into the first band of the spectrum[17] and actually corresponds to one of the smaller peaks. Two higher energies, 7.20 eV for the $^2E''$ state and 7.40 eV for the $^2A''$ state, are within the experimen-

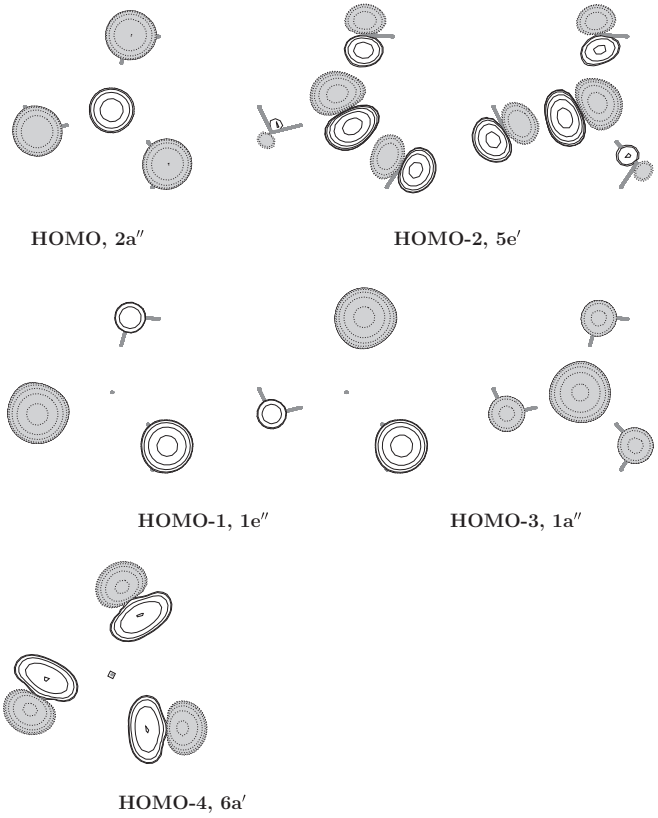

FIG. 9. Canonical Hartree–Fock orbitals of $[F^-(H_2O)_3]$ C_{3h} isomer.

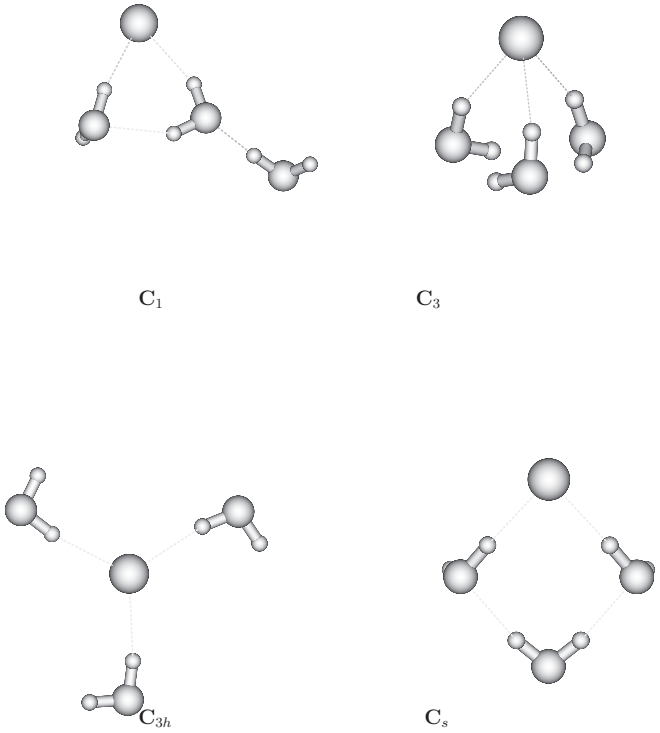

FIG. 10. Isomers of $[Cl^-(H_2O)_3]$.

tal error of the centroid of the second band. The 2a″ orbital is delocalized over all heavy atoms and exhibits antibonding interactions between oxygen and fluorine p_z orbitals (see Fig. 9). Significant delocalization is displayed by all other DOs. Of these, one pair of degenerate MOs, 1e″, does not contain any contribution from the fluorine atom. The orbital with the greatest degree of F 2*p* participation, 1a″, corresponds to the C^2A'' final state.

$[Cl^-H_2O)_3]$

Isomers of the chloride–water trimer were optimized with the MP2 and 6-311++G** and 6-311++G(2*df*,2*p*) basis sets. The results are presented in Table IX and Fig. 10. The two most stable minima correspond to the C_3 and C_s point groups. The third minimum of C_1 symmetry is clearly higher in energy and has only two water molecules that are directly coordinated to the chloride anion.

VEDEs of $[Cl^-H_2O)_3]$ C_3 and C_s structures are presented in Table X. Very good agreement with experiment[15] is achieved by the OVGF method in the C approximation. P3 gives slightly lower energies. The three lowest final states are either identical or almost identical in energy. Corresponding DOs are localized on the chlorine atom; contributions from oxygen orbitals are minor. Three lower lying DOs are formed by H_2O $1b_1$ molecular orbitals with almost no mixing from chlorine orbitals.

TABLE IX. $[Cl^-(H_2O)_3]$ total (a.u.) and relative (kcal/mol) energies.

	MP2/6-311++G**			
Structure	E_{MP2}	ΔE_{MP2}	*i*	ΔE_{ZPE}
C_3	−688.60332	0	0	0
C_{3h}	−688.59632	4.39	4	
C_s	−688.60151	1.13	0	0.73
C_1	−688.59718	3.85	0	1.84
	MP2/6-311++G(2*df*,2*p*)			
Structure	E_{BD}	ΔE_{MP2}	*i*	ΔE_{ZPE}
C_3	−688.78061	0	0	0
C_{3h}	−688.77105	6.00	4	
C_s	−688.77664	2.49	0	1.61
C_1	−688.77314	4.69	0	3.54

TABLE X. $[Cl^-(H_2O)_3]$ VEDEs (eV).

			OVGF				Expt.
Structure	State	KT	A	B	C	P3	Ref. 15
C_3	X^2E	6.14	5.37	5.51	5.53	5.33	5.50
	A^2A	6.18	5.36	5.50	5.52	5.33	
	B^2E	9.43	7.85	8.06	8.07	8.06	
	C^2A	9.72	8.18	8.38	8.40	8.38	
C_s	X^2A'	5.99	5.26	5.41	5.42	5.20	5.50
	A^2A''	6.11	5.33	5.48	5.50	5.30	
	B^2A'	6.11	5.34	5.48	5.50	5.30	
	C^2A'	9.01	7.60	7.82	7.83	7.60	
	D^2A'	9.60	8.09	8.31	8.32	8.08	
	E^2A''	9.67	8.11	8.32	8.34	8.10	

CONCLUSIONS

Electron propagator calculations provide accurate values of the vertical electron detachment energies of complexes that are formed between fluoride or chloride anions with two or three water molecules. Close resemblance has been established between Dyson orbitals and canonical Hartree–Fock orbitals for vertical electron detachment energies of halide–water clusters. Qualitatively different conclusions on the delocalization of the Dyson orbitals have been reached for the fluoride and chloride complexes.

For the chloride–water complexes, delocalization between the chloride and water fragments is negligible in the Dyson orbitals. Therefore, the three lowest final states in these clusters may be classified as having a chlorine atom coordinated to water molecules. The next final state, which is well separated from the former three, constitutes a charge-transfer state in which a chloride anion is juxtaposed with a cationic hole that is delocalized over the water molecules. For chloride–water complexes, anion photoelectron spectra may easily distinguish between final states with a chlorine atom and charge-transfer states where a chloride anion is in the presence of a positively charged array of water molecules.

In the case of fluoride–water clusters, delocalization patterns depend on symmetry. For the C_{2h} and both C_{2v} $[F^-(H_2O)_2]$ clusters, Dyson orbitals pertaining to the first two final states are delocalized over fluorine and oxygen atoms. The third final state is localized on fluorine. Two different patterns are observed for the C and D final states: whereas the C state can be described as a charge transfer to solvent precursor, the D final state is delocalized. In the case of the C_2 isomer, all lower lying Dyson orbitals also are delocalized. Similar conclusions are valid for the isomers of fluoride coordinated to three water molecules. All Dyson orbitals for higher transition energies are delocalized in the final states of the C_3 isomer of $[F^-(H_2O)_3]$. The charge-transfer state, B E″, arises in the C_{3h} isomer of the latter complex.

These results indicate that the Dyson orbitals for VEDEs of solvated fluoride exhibit a degree of delocalization over nearby water molecules that is not found for hydrated chloride anions. They also confirm similar trends that were suggested by preliminary studies of the $F^-(H_2O)$ complex,[20] by a study of aqueous fluoride based on Monte-Carlo generation of solvent configurations[21] and by calculations on hexacoordinate anions embedded in a continuum solvent model.[22] Anion photoelectron spectra of fluoride–water clusters should be assigned in terms of Dyson orbitals that may be delocalized and that reflect the strength of chemical bonding mediated by hydrogen bridges.

ACKNOWLEDGMENTS

This work was supported by National Science Foundation Grant No. CHE-0809199 to Auburn University.

[1] W. H. Robertson and M. A. Johnson, Ann. Rev. Phys. Chem. **54**, 173 (2003).
[2] A. Sanov and W. C. Lineberger, Phys. Chem. Chem. Phys. **6**, 2018 (2004).
[3] M. Mitsui and A. Nakajima, Bull. Chem. Soc. Jpn. **80**, 1058 (2007).
[4] J. Simons, J. Phys. Chem. A **112**, 6401 (2008).
[5] X. Chen and S. Bradforth, Ann. Rev. Phys. Chem. **59**, 203 (2008).
[6] J. Baik, J. Kim, D. Majumdar, and K. S. Kim, J. Chem. Phys. **110**, 9116 (1999).
[7] D. Majumdar, J. Kim, and K. S. Kim, J. Chem. Phys. **112**, 101 (2000).
[8] J. Kim, H. M. Lee, S. B. Suh, D. Majumdar, and K. S. Kim, J. Chem. Phys. **113**, 5259 (2000).
[9] J. E. Combariza and N. R. Kestner, J. Chem. Phys. **100**, 2851 (1994).
[10] J. E. Combariza and N. R. Kestner, J. Phys. Chem. **98**, 3513 (1994).
[11] D. Serxner, C. E. H. Dessent, and M. Johnson, J. Chem. Phys. **105**, 7231 (1996).
[12] C. G. Zhang and D. A. Dixon, J. Phys. Chem. A **108**, 2020 (2004).
[13] D. A. Kemp and M. S. Gordon, J. Phys. Chem. A **109**, 7688 (2005).
[14] G. Markovich, O. Cheshnovsky, and U. Kaldor, J. Chem. Phys. **99**, 6201 (1993).
[15] G. Markovich, S. Pollack, R. Giniger, and O. Cheshnovsky, J. Chem. Phys. **101**, 9344 (1994).
[16] U. Kaldor, Z. Phys. D: At., Mol. Clusters **31**, 279 (1994).
[17] X. Yang, X. B. Wang, and L. S. Wang, J. Chem. Phys. **115**, 2889 (2001).
[18] W. von Niessen, J. Schirmer, and L. S. Cederbaum, Comput. Phys. Rep. **1**, 57 (1984).
[19] I. B. Müller and L. S. Cederbaum, J. Phys. Chem. A **109**, 10424 (2005).
[20] O. Dolgounitcheva, V. G. Zakrzewski, and J. V. Ortiz, Int. J. Quantum Chem. **111**, 1701 (2011).
[21] S. Canuto, K. Coutinho, B. J. C. Cabral, V. G. Zakrzewski, and J. V. Ortiz, J. Chem. Phys. **132**, 214507 (2010).
[22] O. Dolgounitcheva, V. G. Zakrzewski, and J. V. Ortiz, Int. J. Quantum Chem. **112**, 3840 (2012).
[23] J. V. Ortiz, Adv. Quantum Chem. **35**, 33 (1999).
[24] R. Flores-Moreno, J. Melin, O. Dolgounitcheva, V. G. Zakrzewski, and J. V. Ortiz, Int. J. Quantum Chem. **110**, 706 (2010).
[25] V. G. Zakrzewski, O. Dolgounitcheva, A. V. Zakjevskii, and J. V. Ortiz, in *Advances in Quantum Chemistry*, edited by J. R. Sabin and E. Brändas (Elsevier, Amsterdam, 2011), Vol. 62, p. 105.
[26] J. V. Ortiz, WIREs Comput. Mol. Sci. **3**, 123 (2013).
[27] N. C. Handy, J. A. Pople, M. Head-Gordon, K. Raghavachari, and G. Trucks, Chem. Phys. Lett. **164**, 185 (1989); C. E. Dykstra, *ibid.* **45**, 466 (1977).
[28] M. J. Frisch, G. W. Trucks, H. B. Schlegel *et al.*, GAUSSIAN, Developers' Version, Revision H.01, Gaussian, Inc., Wallingford, CT, 2008.
[29] R. Krishnan, J. S. Binkley, R. Seeger, and J. A. Pople, J. Chem. Phys. **72**, 650 (1980); M. J. Frisch, J. A. Pople, and J. S. Binkley, *ibid.* **80**, 3265 (1984).
[30] J. V. Ortiz in *Computational Chemistry: Reviews of Current Trends*, edited by J. Leszczynski (World Scientific, Singapore, 1997), Vol. 2, p. 1.
[31] J. V. Ortiz, J. Chem. Phys. **104**, 7599 (1996).
[32] A. M. Ferreira, G. Seabra, O. Dolgounitcheva, V. G. Zakrzewski, and J. V. Ortiz, in *Quantum-Mechanical Prediction of Thermochemical Data*, edited by J. Cioslowski (Kluwer, Dordrecht, 2001), p. 131.
[33] J. V. Ortiz, Int. J. Quantum Chem. **105**, 803 (2005).
[34] G. Schaftenaar, MOLDEN, version 3.4, CAOS/CAMM Center, The Netherlands, 1998.